Tuning the solution self-assembly of a peptide-PEG (polyethylene glycol) conjugate with alpha-cyclodextrin

ChemBioChem

Research Article
doi.org/10.1002/cbic.202300472

Chemistry Europe
European Chemical Societies Publishing

www.chembiochem.org

Special Collection

Tuning the Solution Self-Assembly of a Peptide-PEG (Polyethylene Glycol) Conjugate with α-Cyclodextrin

Valeria Castelletto,*[a] Radoslaw M. Kowalczyk,[a] Jani Seitsonen,[b] and Ian W Hamley*[a]

Cyclodextrins are saccharide ring molecules which act as host cavities that can encapsulate small guest molecules or thread polymer chains. We investigate the influence of alpha-cyclodextrin (αCD) on the aqueous solution self-assembly of a peptide-polymer conjugate YYKLVFF-PEG3K previously studied by our group [Castelletto *et al.*, *Polym. Chem.*, 2010, 1, 453–459]. This conjugate comprises a designed amyloid-forming peptide YYKLVFF that contains the KLVFF sequence from Amyloid β peptide, Aβ16-20, along with two aromatic tyrosine residues to enhance hydrophobicity, as well as polyethylene glycol PEG with molar mass 3 kg mol^{-1}. The conjugate self-assembles into β-sheet fibrils in aqueous solution. Here we show that complexation with αCD instead generates free-floating nanosheets in aqueous solution (with a β-sheet structure). The nanosheets comprise a bilayer with a hydrophobic peptide core and highly swollen PEG outer layers. The transition from fibrils to nanosheets is driven by an increase in the number of αCD molecules threaded on the PEG chains, as determined by ^{1}H NMR spectroscopy. These findings point to the use of cyclodextrin additives as a powerful means to tune the solution self-assembly in peptide-polymer conjugates and potentially other polymer/biomolecular hybrids.

Introduction

Control of self-assembly through judicious use of non-covalent interactions is an important theme in contemporary materials chemistry research.[1] Cyclodextrins are model compounds that comprise small rings of saccharide units (6, 7, and 8 in αCD, βCD and γCD respectively) and molecular size cavities that form rotaxanes in complexation with polymers (inclusion complexes).[2] As water soluble molecules able to form host-guest complexes, cyclodextrins have been widely explored for applications in pharmaceutics since they can be used to create water-soluble complexes with hydrophobic drugs.[3] In addition, they have a very extensive range of applications in the food, cosmetic, and personal care industries and in the formulation of pesticides for agriculture, among others.[4] These simple cyclic carbohydrates with toroid-like structures are readily available commercially and have been shown to thread around different molecular chains including polymers and alkyl chains, depending on the size of the cyclodextrin ring (and hence cavity size) and its hydrophobicity/hydrophilicity. This can influence self-assembly due to the changes in molecular packing that result from inclusion complex formation, as demonstrated for example for surfactants[5] or copolymers such as those containing PEG,[6] among other systems. Among cyclodextrins, αCD contains six glucose-derived saccharides and contains a small hydrophobic cavity, which can thread around polymers including polyethylene glycol (PEG).[7]

Conjugation of poly(ethylene glycol) PEG to peptides may be useful in therapeutic applications since PEG confers extended stability to peptide structures *in vivo* due to steric stabilization by PEG chains, as well as the increased mass which hinders rapid elimination from the body.[8] In addition, attachment of PEG which is hydrophilic to hydrophobic peptides produces amphiphilic molecules which can self-assemble into nanostructures such as fibrils, and at sufficiently high concentration liquid crystal structures We have previously examined the self-assembly of PEG-peptides containing designed amyloid peptide fragments based on a core motif from the Amyloid β (Aβ), KLVFF (Aβ16-20)[9] in which the aromatic FF dipeptide motif is believed to play an essential role in driving β-sheet formation through aromatic stacking interactions. We observed self-assembly into fibrils, and lyotropic liquid crystal phase formation at high concentration, including nematic and hexagonal columnar phases.[10] We have examined this for FFKLVFF-PEG with PEG3K (i.e. polyethylene glycol with molar mass $M_w = 3$ kg mol^{-1}). This construct contains a dipeptide FF dipeptide extension of the core KLVFF peptide. We also studied the self-assembly of the corresponding non-PEGylated AAKLVFF and FFKLVFF peptides in methanol.[11] and for AAKLVFF in water and water/methanol mixtures.[12] We later investigated the influence of PEG molar mass on the self-assembly of FFKLVFF-PEG with PEG with molar mass of 1000 g mol^{-1}, 2000 g mol^{-1}, and 10,000 g mol^{-1}.[10c,d]

[a] Dr. V. Castelletto, Dr. R. M. Kowalczyk, Prof. Dr. I. W Hamley
School of Chemistry, Food Biosciences and Pharmacy
University of Reading
Whiteknights, Reading RG6 6AD (UK)
E-mail: v.castelletto@reading.ac.uk
i.w.hamley@reading.ac.uk

[b] Dr. J. Seitsonen
Nanomicroscopy Center, Aalto University
Puumiehenkuja 2, 02150 Espoo (Finland)

Supporting information for this article is available on the WWW under https://doi.org/10.1002/cbic.202300472

Special Collection This article is part of the Special Collection "Peptide-Based Supramolecular Systems". Please see our homepage for more articles in the collection.

We previously showed that YYKLVFF-PEG (with PEG1K or PEG3K) forms fibrils in aqueous solutions (and nematic and columnar phases at high concentration).[10d] Here, we investigate the influence of αCD on the aqueous solution self-assembly of YYKLVFF-PEG3K. Self-assembly is investigated using both cryo-TEM imaging and small-angle x-ray scattering (SAXS) and the peptide secondary structure was probed using FTIR and ThT fluorescence experiments to confirm β-sheet content. We find that addition of αCD has a dramatic influence on the nanostructure. Whereas fibrils are formed by YYKLVFF-PEG3K, addition of αCD at a sufficient concentration leads to self-assembly into free-floating nanosheets.

Experimental Section

Materials. α-cyclodextrin (αCD) (Scheme 1) was obtained from Sigma-Aldrich (UK). The PEGylated conjugate YYKLVFF-PEG3K (Scheme 1) was synthesized by Rapp Polymere GmbH using solid phase peptide synthesis methods. PEGylated TentaGel PAP resin was used, which comprises porous PS beads to which PEG is attached via acid cleavable linkages. The peptide was assembled from the C-terminus towards the N-terminus, and was attached to the solid support at the C-terminus via the α-carbonyl group of the amino acid. The crude peptide was characterized by reverse phase high performance liquid chromatography (RP-HPLC; Grom Saphir 200, C18 5 mm column). A mobile phase with a gradient of water with 0.1% TFA and acetonitrile with 0.75% TFA was used. Sample elution was monitored using a UV/vis detector operating at 220 nm. MALDI-TOF (Ultraflex, Bruker with matrix Universalmatrix, Fluka) was used to confirm $M_n = 4110\ g\,mol^{-1}$ for YYKLVFF-PEG3K, consistent with addition of YYKLVFF (Mn = 979.2 g mol^{-1}, expected) to the precursor PEG (Mn = 3139 g mol^{-1}, MALDI-TOF, 3060 g mol^{-1} GPC). GPC (eluent: THF) of the starting PEG3K indicates low polydispersity $M_w/M_n = 1.05$.

Samples were prepared by mixing weighed amounts of the peptide powder with weighed amounts of the corresponding ready prepared αCD solutions. Images showing the appearance of samples in vials are provided in SI Figure S1.

Nuclear Magnetic Resonance (NMR) All NMR spectra were recorded on 700 MHz Bruker Avance spectrometer (16.445 T) at room temperature (297 K), equipped with a high-sensitivity TCI cryoprobe. The standard zg30 pulse sequence was used with 1 s relaxation delay and 1024 FID transients were accumulated and processed into spectra with 0.064 Hz resolution. Chemical shifts were referenced to the residual solvent (DMSO-d_6) signal at 2.50 ppm. The phase and baseline of each spectrum were corrected, and resonances integrated using TopSpin 3.5 Bruker software.

The structures of YYKLVFF-PEG3K and αCD were verified using parameters collected in Supplementary Table S1 using the intensity ratio formula: $(I^A/I^B) * N_p^B * (M_w^A/M_w^B) * (wt\%^B/wt\%^A)$, where I denotes intensity of the relevant NMR resonance, N_p is the number of protons contributing to this resonance, M_w is molecular weight and wt% is the concentration of the compound in the measured NMR sample. The number of αCD molecules threading the PEG chain in YYKLVFF-PEG3K was estimated directly from the ratio of

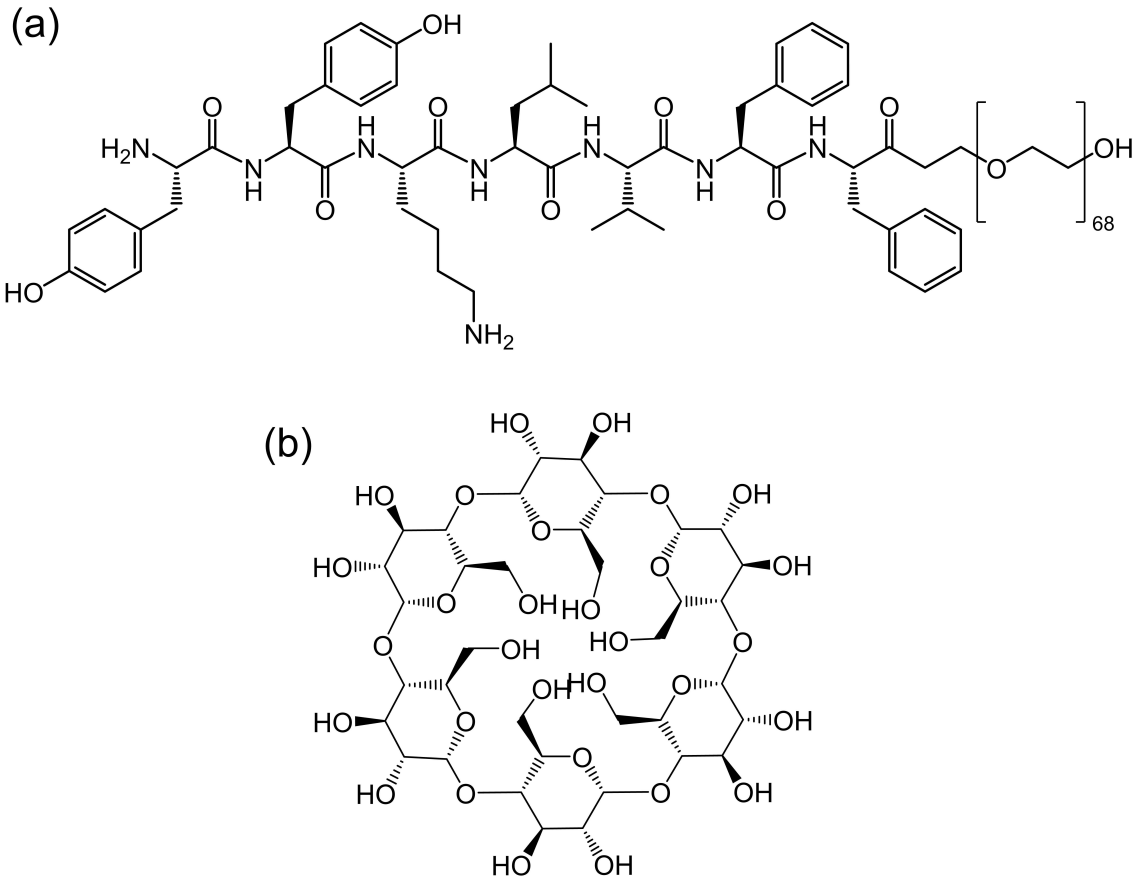

Scheme 1. Molecular structures. (a) YYKLVFF-PEG3K (average degree of polymerization $n = 68$ indicated), (b) α-cyclodextrin.

intensities of the resonances at 3.51 ppm (YYKLVFF-PEG3K) and 4.79 ppm (αCD) using the formula $(N_p^{PEG}/N_p^{\alpha CD})*(I^{\alpha CD}/I^{PEG})$ where it was assumed $N_p^{PEG}=272$ and $N_p^{\alpha CD}=6$ and the relevant intensities are listed in Table S1. Experimental errors were estimated applying Taylor's method to the relevant formula. The source of the largest intensity errors is due to the quality of DMSO-d_6 (8%) and overlap of other unresolved signals especially with the 3.51 ppm resonance (6%). These overlaped resonances origiante most likely from protons which link PEG with the peptide chain.

Fluorescence spectroscopy. Experiments were carried out using a Varian Model Cary Eclipse spectrofluorometer. Solutions were loaded in a 10 mm light path quartz cell. Thioflavin T (ThT) fluorescence assays were performed to identify the possible formation of β-sheet structures in samples containing YYKLVFF-PEG3K or mixtures of PEGylated peptide with αCD. For the experiments, samples were prepared using a solution of 5.0×10^{-3} wt % ThT as a solvent. To keep consistency with other experiments, samples were initially prepared with 1 wt% YYKLVFF-PEG3K, with 0, 0.5, 1, 5 or 10 wt% αCD. These solutions were then diluted 7-fold to allow for fluorescence experiments. The fluorescence of ThT was excited at 440 nm and the emission spectra were measured from 460 to 800 nm.

Fourier Transform Infrared (FTIR) Spectroscopy. Spectra were recorded using a Thermo-Scientific Nicolet iS5 instrument equipped with a DTGS detector, with a Specac Pearl liquid cell (samples in D_2O contained between fixed CaF_2 plates). Spectra were scanned 116 times over the range 900–4000 cm^{-1}.

Cryogenic-TEM (Cryo-TEM). Imaging was carried out using a field emission cryo-electron microscope (JEOL JEM-3200FSC), operating at 200 kV. Images were taken in bright field mode and using zero loss energy filtering (omega type) with a slit width of 20 eV. Micrographs were recorded using a Gatan Ultrascan 4000 CCD camera. The specimen temperature was maintained at −187 °C during the imaging. Vitrified specimens were prepared using an automated FEI Vitrobot device using Quantifoil 3.5/1 holey carbon copper grids with a hole size of 3.5 μm. Just prior to use, grids were plasma cleaned using a Gatan Solarus 9500 plasma cleaner and then transferred into the environmental chamber of an FEI Vitrobot at room temperature and 100% humidity. Thereafter, 3 μl of sample solution was applied on the grid which was blotted twice for 5 seconds and then vitrified in a 1/1 mixture of liquid ethane and propane at temperature of −180 °C. The grids with vitrified sample solution were maintained at liquid nitrogen temperature and then cryo-transferred to the microscope.

Small-Angle X-Ray Scattering (SAXS) Synchrotron SAXS experiments on solutions were performed using BioSAXS robots on beamline B21[13] at Diamond (Didcot, UK), or BM29 at the ESRF (Grenoble, France).[14] A few microlitres of each sample were injected via an automated sample exchanger at a slow and very reproducible rate into a quartz capillary (1.8 nm internal diameter), in the X-ray beam. The quartz capillary was enclosed in a vacuum chamber to avoid parasitic scattering. After the sample was injected into the capillary and reached the X-ray beam, the flow was stopped during the SAXS data acquisition. Samples containing mixtures of YYKLVFF-PEG3K with 5 and 10 wt% αCD were slightly viscous and, at Diamond, were loaded into poly(ethyleneimine) capillaries mounted into the multipurpose sample cell.[15] At Diamond, the q range was set to 0.007–0.33$Å^{-1}$, with wavelength $\lambda=0.95Å$. The images were captured using a Pilatus 1 M detector. At the ESRF the q range was 0.005–0.48$Å^{-1}$, with $\lambda=1.03Å$, and the images were obtained using a Pilatus Pilatus3-2M detector. Data processing (background subtraction, radial averaging) was performed using dedicated beamline software iSPyB or ScatterIV at the ESRF or Diamond respectively.

SAXS fitting models. Depending on the sample composition, the SAXS data was fitted using SASfit[16] with form factors containing contributions of long cylindrical shells, generalized Gaussian coils, or homogeneous plates.[17] The long cylindrical shell model parameters are the polydisperse core radius, R, the thickness of the cylindrical shell, Δ_R, the length of the cylinders, L, and the scattering length density of core, η_c, shell, η_s and solvent, η_{so}. The generalized Gaussian coils are described by the Guinier radius, R_{gG}, and the Flory exponent, ν. The parameters for the homogeneous plate form factor are polydisperse layer thickness, T, and the diameter of the planar object, D. Where present, structure factor was fitted using a Lorentzian function, with amplitude A; position of peak maximum q_0; width W and background BG.

Results

We first used ^{1}H NMR to determine the average number of αCD molecules threading a PEG chain. Molecular characteristics are listed in SI Table S1 and Table 1 contains data from the ^{1}H NMR spectra for samples containing 0, 0.5, 2.5, and 5 wt% αCD. The spectra are shown in SI Figures S2 and S3. Two sets of experiments were run for samples 0.5% YYKLVFF-PEG3K: 2.5% αCD, with and without added TFA-*d* which was added in case any YYKLVFF-PEG3K aggregation caused NMR-silent species. In fact, very similar results were obtained with and without TFA-*d* which shows the absence of such species. The results in Table 1 show a significant increase in the number of αCD threaded

Table 1. Structure verification data obtained from ^{1}H NMR. Estimated errors are given in parentheses.

Sample	Number of PEG monomers in YYKLVFF-PEG3K	Number of saccharides in αCD	Number of αCD per YYKLVFF-PEG3K chain, $n_{\alpha CD}$
0.5 wt% YYKLVFF-PEG3K	73(10)		
0.5 wt% YYKLVFF-PEG3K + TFA-*d*	64(9)		
2.5 wt% αCD		7(1)	
2.5 wt% αCD + TFA-*d*		5(1)	
0.5 wt% YYKLVFF-PEG3K: 0.5% αCD	73(10)	7(1)	4(1)
0.5 wt% YYKLVFF-PEG3K: 2.5% αCD	81(11)	7(1)	19(5)
0.5 wt% YYKLVFF-PEG3K: 2.5 wt% αCD + TFA-*d*	64(9)	5(1)	20(5)
0.5 wt% YYKLVFF-PEG3K: 5.0% αCD	80(11)	7(1)	39(10)

molecules on each PEG chain in YYKLVFF-PEG3 K as the αCD content increases. Figure S2 shows a comparison of spectra for αCD and a solution containing 0.5% YYKLVFF-PEG3K and 0.5%, 2.5%, and 5.0% αCD, respectively. The resonances in YYKLVFF-PEG3 K: αCD are broadened and shifted which is attributed to interaction between αCD and PEG, in agreement with a prior study on PEG-αCD complexes.[18] The lesser extent of the line broadening (especially for 0.5% YYKLVFF-PEG3K: 2.5% αCD) is possibly because of better quality spectra obtained at higher frequency spectrometer (700 vs 400 MHz). However, it is necessary to stress that the "broadening" itself does not unambiguously prove that all αCD are threaded on the YYKLVFF-PEG3K. There are two reasons for this: firstly, all resonances for a "free" and threaded αCD molecule have nearly identical chemical shifts and would thus completely overlap in the solution (see SI Figure S2). This is particularly problematic for the cases where there is a modest difference between content of both species in the solution because the resulting resonance would have a linewidth which is a combination of the linewidth of both species. Secondly, the resonances of the -OH groups (e.g. 5.51 ppm, 5.43 ppm, and 4.48 ppm) undergo a slow proton – deuteron exchange, which allows their detection in the NMR spectrum but any change in the rate of this exchange will contribute to the change of the linewidth. SI Figure S3 shows the ^{1}H spectra of 0.5% YYKLVFF-PEG3 K with 0.5% αCD, 2.5% αCD, 2.5% αCD with TFA-*d*, and 5.0% αCD.

The ratio of relative resonance intensities ($I^{\alpha CD}$ /I^{PEG}) obtained from the ^{1}H NMR spectra allows the number of αCD molecules per YYKLVFF-PEG3K chain to be determined, as listed in Table 1. This shows that there is a significant increase in the number of threaded αCD molecules with an increase in αCD content in the complexes from $n_{\alpha CD}=4$ for 0.5 wt% αCD to $n_{\alpha CD}=39$ for 5 wt% αCD. The value for 2.5 wt% αCD, $n_{\alpha CD}=19$ may be compared to the value obtained with TFA-*d* which is very similar, $n_{\alpha CD}=20$. This indicates the lack of NMR-silent aggregates. Both values, in regard to the preceding discussion, should be considered as an upper limit of αCD molecules threaded on the YYKLVFF-PEG3K chain. It is noted that all –OH peaks in the spectrum have disappeared due to exchange with NaOD (SI Figure S2). Our results for the complex containing 2.5 wt% αCD are in exact agreement with those of Peña-Bahamonde *et al.* ($n_{\alpha CD}=19$ for PEG3K),[19] but indicate a higher extent of αCD threading for our 0.5 wt% αCD complexes (lower for 0.25 wt% αCD complexes) than reported for aggregate-rich precipitates of PEG1.5K with αCD.[20]

FTIR was used to probe the secondary structure, through analysis of peaks in the amide I region. The spectra in Figure 1a show the presence of a peak at 1626 cm^{-1} for all samples. This peak can be ascribed to β-sheet structure[21] and the data indicate the persistence in solution of β-sheet structure within the peptide component of YYKLVFF-PEG3K for the conjugate itself and in solutions with up to 10 wt% added αCD (i.e. across the range studied). Although αCD itself has been reported to show an FTIR band at 1638 cm^{-1},[22] we did not find evidence for such a peak (SI Figure S4). The spectra in Figure 1b show peaks due to CH_2/CH_3 symmetric and asymmetric stretch deformations[23] and peaks at 2883 and 2923 cm^{-1} are retained for all samples, although with significantly increased absorbance for 5 and 10 wt% αCD. These peaks are mainly due to the predominant CH_2 groups in the PEG ethers, although αCD has been reported to have a peak at 2923 cm^{-1},[22] and indeed a peak close to this at 2936 cm^{-1} was observed, as well as a shoulder peak at 2883 cm^{-1} (SI Figure S4). The enhancement of these CH_2/CH_3 deformation mode peaks in the complexes with αCD reflects binding of more αCD with the PEG chains upon increase of αCD content.

Thioflavin T (ThT) is a fluorescent dye which is a sensitive probe of 'amyloid' β-sheet formation.[21c,24] We used fluorescence with ThT as a further test of β-sheet formation in the YYKLVFF-PEG3K complexes with αCD. The corresponding spectra and analysis of the peak height are shown in Figure 2. The data clearly show fluorescence well above the control (blank) for YYKLVFF-PEG3K, and although the peak intensity is slightly reduced for YYKLVFF-PEG3K/αCD complexes, it is still significantly above the level for the controls (αCD only with ThT) as is clear from the data in Figure 2b. These data provide additional evidence that β-sheet structure is retained in all YYKLVFF-PEG3K/αCD complexes studied.

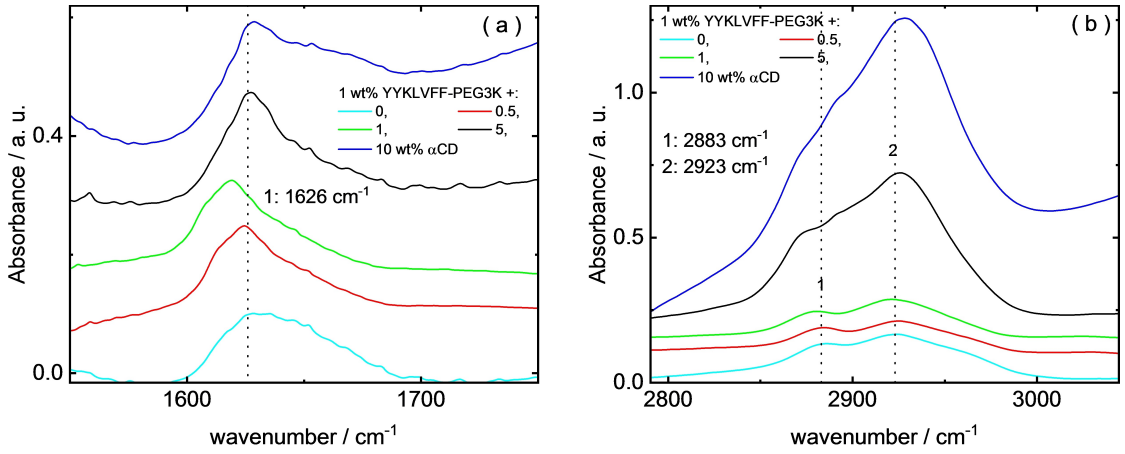

Figure 1. FTIR spectra for samples containing 1 wt% YYKLVFF-PEG3K with 0–10 wt% αCD. (a) Amide I/II region (b) Region of CH_2/CH_3 stretch deformations. The FTIR spectra have been shifted vertically, and the intensity of the data in (b) for 0.5 wt% αCD has been multiplied by 10, to allow for visualization.

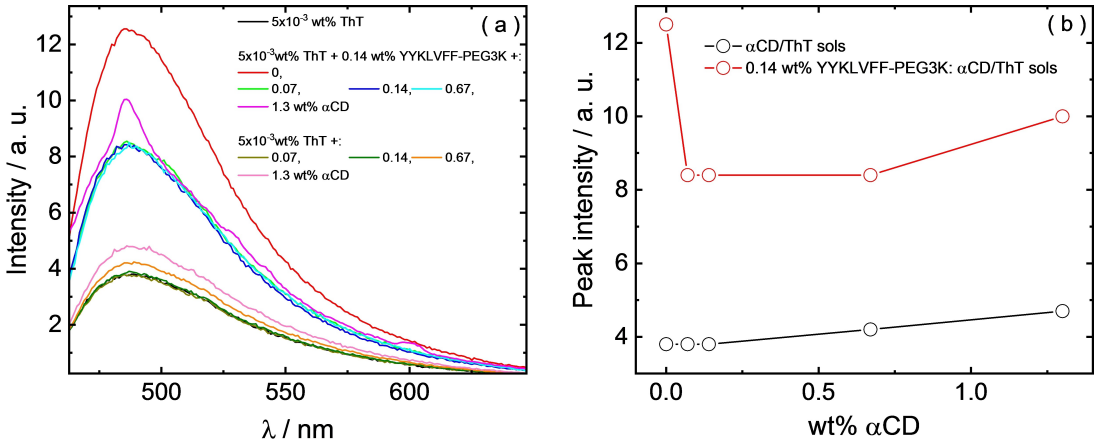

Figure 2. (a) ThT fluorescence curves and (b) Intensity maximum for the data in (a) as a function of wt% αCD.

Cryo-TEM was used to image vitrified sample solutions. Representative images are shown in Figure 3. YYKLVFF-PEG itself forms short fibrils as evident from Figure 3a. Fibrils are still observed upon addition of 1 wt% αCD (Figure 3b), although

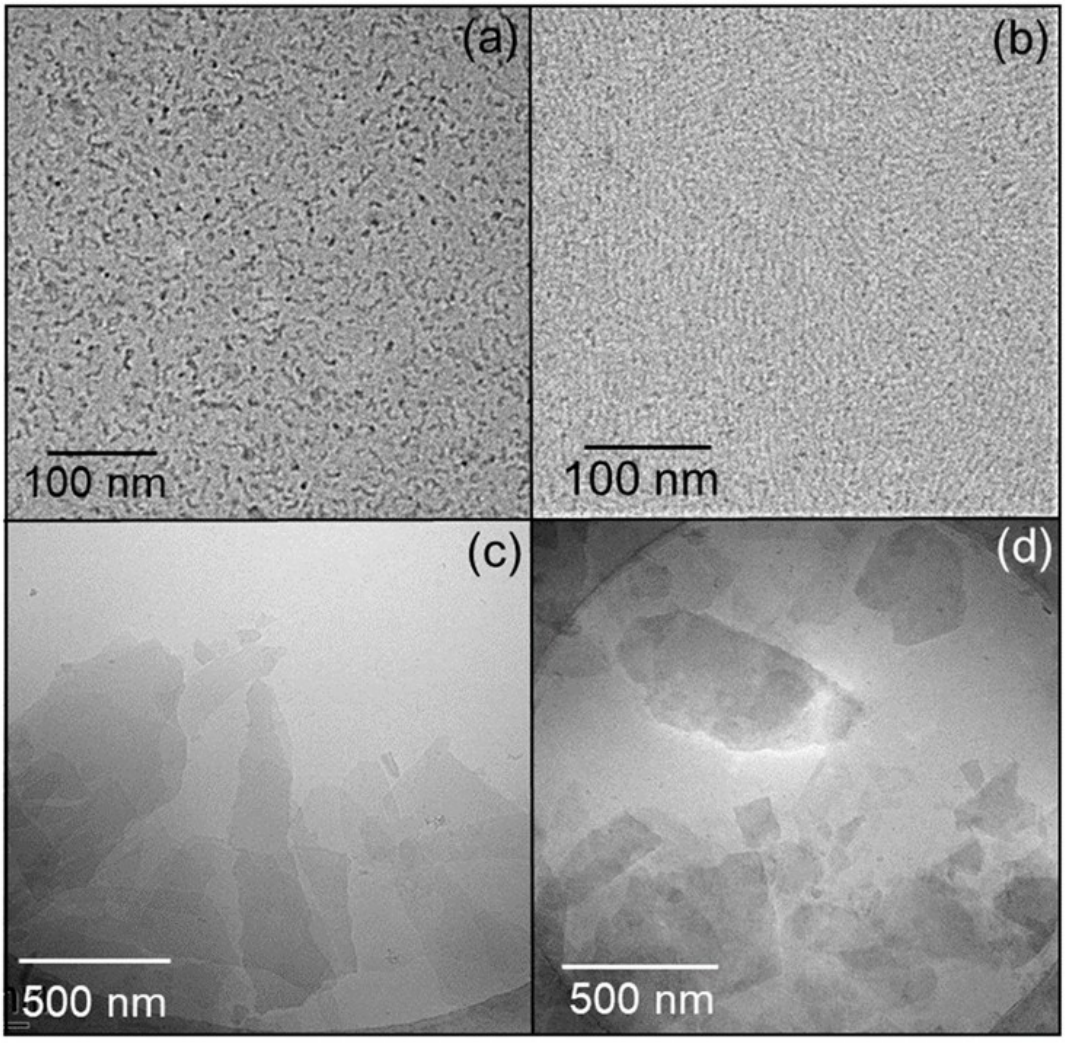

Figure 3. Cryo-TEM images obtained for 1 wt% YYKLVFF-PEG3K with (a) 0, (b) 1, (c) 5, and (d) 10 wt% αCD.

they are more extended than for the peptide-PEG conjugate itself (extended fibrils and aligned fibrils were notable for YYKLVFF-PEG3K at higher concentration in our previous report[10d]). Increasing the αCD content leads to very distinct nanostructures. As evident from Figure 3c,d, large nanosheets or platelets (with a range of widths) are observed for the solutions based on complexes containing 5 or 10 wt% αCD. Consistent with the presence of large nanosheets, the appearance of the samples changes, becoming cloudy for the solutions containing 5 or 10 wt% αCD as shown in SI Figure S1.

The SAXS data obtained for the solutions of YYKLVFF-PEG3K and complexes with αCD is shown in Figure 4. This provides sample-averaged information on the size and shape of self-assembled nanostructures through form factor analysis.[17] The fitted form factor parameters are listed in SI Table S2 and S3. The data for YYKLVFF-PEG3K itself can be fitted to a core-shell cylinder form factor (with an additional sloping background which allows for the presence of some clusters of fibrils and/or unassociated conjugate molecules). The fibril core radius is 3.63 nm with a shell thickness of 0.56 nm, giving a total fibril diameter of 8.4 nm, in good agreement with the cryo-TEM images in Figure 3. The SAXS data for the complexes containing 0.1 wt% and 1 wt% αCD required consideration of an additional term in the form factor to fit the data, in particular a contribution from αCD monomers (represented as small 'coils', see also SI Figure S5 which shows the SAXS data for two αCD solutions, with fit parameters in SI Table S4). The main core-shell cylinder form factor fit parameters (SI Table S2) indicate a

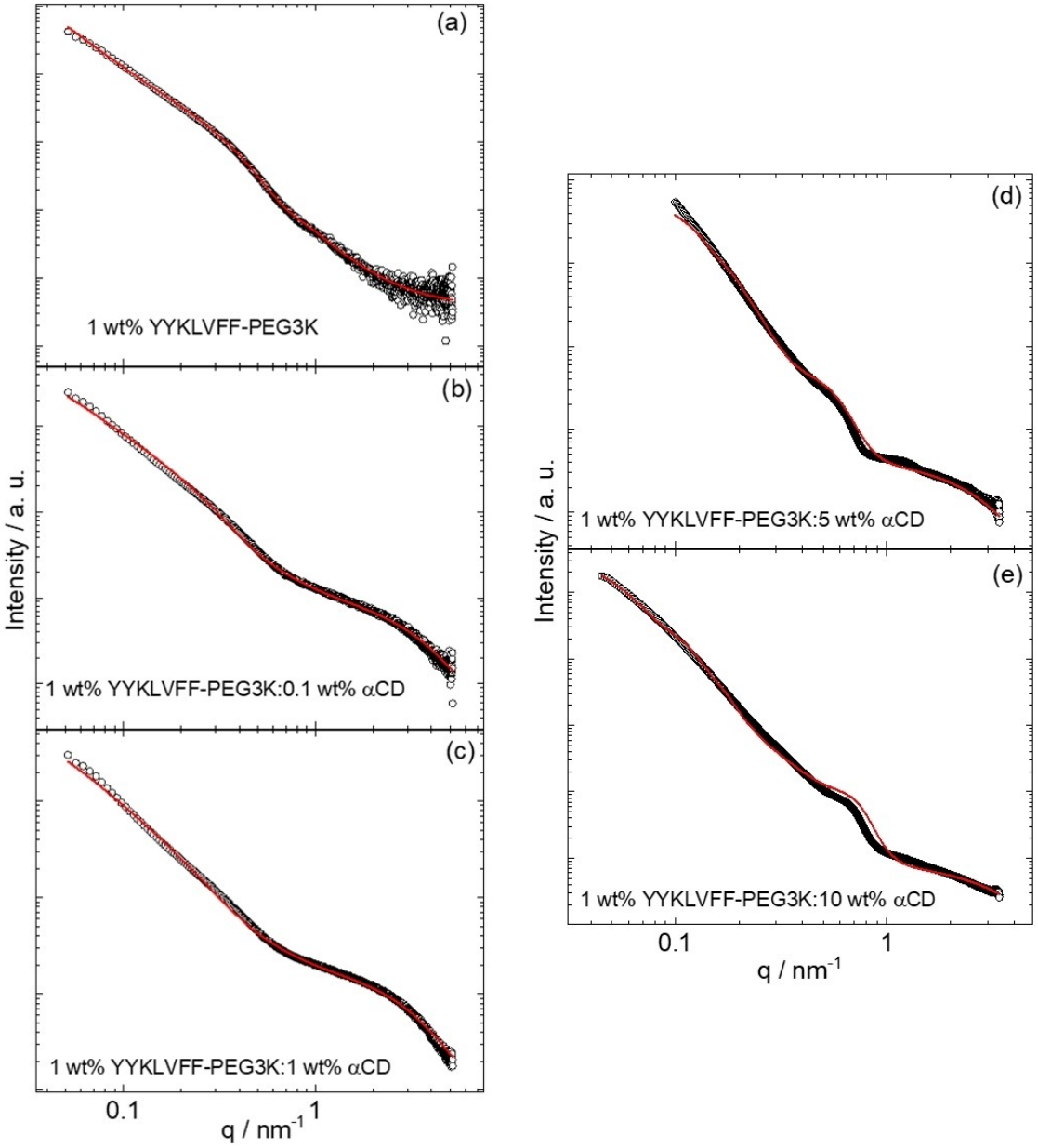

Figure 4. SAXS data (open symbols) and model fits (red lines) as described in the text for 1 wt% YYKLVFF-PEG3K with (a) 0, (b) 0.1, (c), 1, (d) 5, and (e) 10 wt % αCD. The fitted parameters are listed in Tables S1 and S2.

reduction in the cylinder core radius with increase of αCD content, we believe this reflects changes in the core/shell contrast as more αCD molecules thread the PEG chain rather than an actual reduction in the radius of the core which must comprise the hydrophobic YYKLVFF peptide. In contrast to the data for the three lowest αCD complexes studied, the SAXS data for the solutions containing YYKLVFF-PEG3K with 5 or 10 wt% αCD shows distinct features: (i) the slope of the intensity profile is increased at low q (to $I{\sim}q^{-3}$ approximately), (ii) a broad peak develops near $q = 0.6$ nm^{-1} which is enhanced for the solution containing 10 wt% αCD. This data can be fitted consistent with the observations from cryo-TEM (Figure 3c,d) of nanosheet structures, and a form factor for a uniform sheet structure was used to fit the data, also allowing for a contribution from αCD monomers not bound to the PEG (represented as 'coils') and a sloping background. This provides good quality fits and the model indicates single bilayer nanosheets with layer thicknesses $T = 154$ Å for 1 wt% YYKLVFF-PEG3K + 5 wt% αCD and $T = 209$ Å for 1 wt% YYKLVFF-PEG3K + 10 wt% αCD (Table S3).

Discussion and Conclusions

We have shown through cryo-TEM and SAXS that loading of αCD leads to a change in morphology from fibrils to nanosheets in solutions containing complexes of YYKLVFF-PEG with high αCD content. FTIR and ThT fluorescence data show the retention of β-sheet structure.

The SAXS data indicates that the nanosheets comprise single bilayers since there is no evidence for structure factor peaks from a multilayer structure. The estimated radius of gyration of PEG[25] with $M_w = 3140$ g mol^{-1} (degree of polymerization $n = 72$) is $R_g = 19.4$ Å which, even considering the extra size of the YYKLVFF peptide, is clearly much lower than the nanosheet thickness determined from SAXS (154 Å for the 5 wt % αCD solution and 209 Å for the solution with 10 wt% αCD). In fact, these thickness values point to the stretching of the PEG chains caused by αCD threading. The chain length of PEG in an extended conformation can be estimated as $l_{PEG}/\text{Å} = 0.95\ z_E$ where z_E is the number of chain atoms (C and O),[26] which for PEG3K gives $l_{PEG} = 205$ Å. Adding in the estimated length of YYKLVFF in a parallel β-sheet structure[27] ($l_{peptide} = 7 \times 3.2 = 22.4$ Å) leads to a total extended length for the conjugate $l = l_{PEG} + l_{peptide} = 227$ Å. This may be compared to half the total thickness $T/2$ (corresponding to one layer, i.e. half the bilayer structure of a nanosheet) obtained from our SAXS data for the YYKLVFF-PEG/αCD solution containing 10 wt% αCD, $T/2 = 104$ Å. This indicates highly swollen PEG chains, although they are not fully extended. The value for the solution containing 5 wt% αCD is lower, indicating a less extended conformation for this case with fewer αCD chains threaded on the PEG chain. The SAXS data and cryo-TEM images therefore indicate nanosheets comprising highly swollen PEG chains, constrained by αCD threading as shown schematically in Figure 5. These findings may be compared with the results of Uenuma *et al.* on PEG threaded by αCD (pseudo-polyrotaxanes in their notation) which they showed leads to nanosheet self-assembly.[7d] They present SAXS data for several low molar mass PEG samples with αCD, and from form factor fitting obtained a layer thickness $T = 255$ Å for an aqueous solution of the complex with PEG3.4K. Considering the quality of the presented fits (polydispersity was not considered) this can be considered to be in good agreement with the values obtained here (Table S3).

In summary, threading of αCD on PEG chains in the conjugate YYKLVFF-PEG3K drives a transition in self-assembled morphology from fibrils to nanosheets at sufficiently high αCD content. Proton NMR shows a significant increase in the number of αCD molecules threaded per PEG chain as the αCD content increases. This presumably changes the molecular packing and highly threaded PEG chains favour a planar structure. The nanosheets comprise highly swollen bilayers, with a YYKLVFF hydrophobic peptide core and with extended PEG chains in the outer layers due to αCD threading. The PEG is highly extended, i.e. it is super-swollen to as much as five times its Gaussian coil radius of gyration. These findings show that αCD can be used to tune self-assembly in PEGylated biomolecules and that cyclodextrin threading leads to swelling of PEG chains. This represents a valuable tool in the non-covalent modification of PEG conjugate nanostructures that could also be extended to prepare swollen PEG brushes at surfaces among other applications.

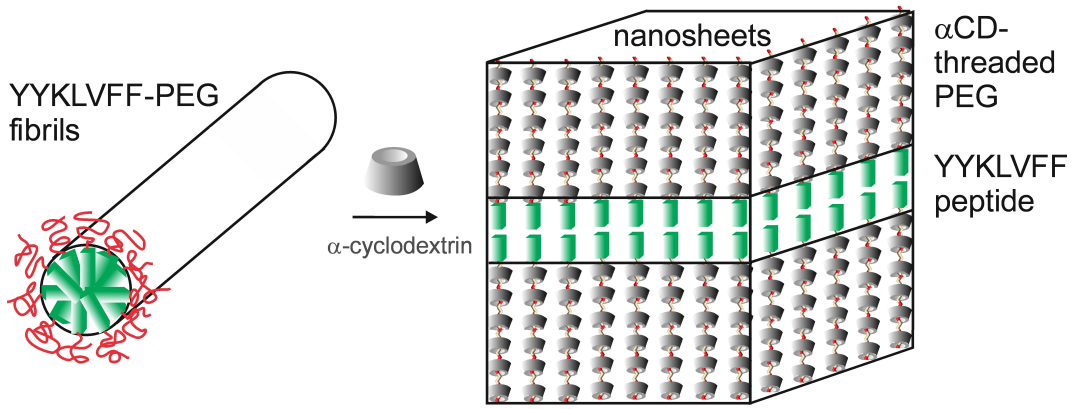

Figure 5. Scheme showing transition from fibrils of YYKLVFF-PEG3K to nanosheets with αCD threaded extended PEG chains.

Supporting Information

Images of samples in vials, NMR spectra, FTIR spectra for αCD, SAXS data for αCD, Tables of SAXS fit parameters

Acknowledgements

This work was supported by an EPSRC Fellowship grant (reference EP/V053396/1) to IWH. We thank Diamond for the award of SAXS beamtime on B21 (references SM29895-1 and SM26698-18) and Nikul Khunti and Charlotte Edwards-Gayle for assistance and the ESRF for beamtime on BM29 (ref. MX-2513) and Mark Tully and Dihia Moussaoui for help. We acknowledge the use of facilities in the Chemical Analysis Facility (CAF) at the University of Reading.

Conflict of Interests

The authors declare no conflict of interest.

Data Availability Statement

The data that support the findings of this study are available from the corresponding author upon reasonable request.

Keywords: cyclodextrins · PEG · peptide conjugates · rotaxanes · self-assembly

[1] T. Aida, E. W. Meijer, S. I. Stupp, *Science* **2012**, *335*, 813–817.
[2] G. Wenz, B. H. Han, A. Muller, *Chem. Rev.* **2006**, *106*, 782–817.
[3] a) T. Loftsson, M. E. Brewster, *J. Pharm. Sci.* **1996**, *85*, 1017–1025; b) K. Uekama, F. Hirayama, T. Irie, *Chem. Rev.* **1998**, *98*, 2045–2076; c) M. E. Davis, M. E. Brewster, *Nature Rev. Drug Dis.* **2004**, *3*, 1023–1035; d) E. M. M. Del Valle, *Process Biochem.* **2004**, *39*, 1033–1046; e) M. E. Brewster, T. Loftsson, *Adv. Drug Delivery Rev.* **2007**, *59*, 645–666; f) T. Loftsson, D. Duchene, *Int. J. Pharmaceut.* **2007**, *329*, 1–11.
[4] J. Szejtli, in *Inclusion Compounds, Volume 3 Physical Properties and Applications, Vol. 3* (Eds.: J. L. Attwood, J. E. D. Davies, D. D. MacNicol), Academic Press, London, **1984**.
[5] a) L. X. Jiang, Y. Peng, Y. Yan, M. L. Deng, Y. L. Wang, J. B. Huang, *Soft Matter* **2010**, *6*, 1731–1736; b) C. C. Tsai, W. B. Zhang, C. L. Wang, R. M. Van Horn, M. J. Graham, J. Huang, Y. M. Chen, M. M. Guo, S. Z. D. Cheng, *J. Chem. Phys.* **2010**, *132*; c) L. D. S. Araujo, L. Watson, D. A. K. Traore, G. Lazzara, L. Chiappisi, *Soft Matter* **2022**, *18*.
[6] a) J. Li, X. P. Ni, Z. H. Zhou, K. W. Leong, *J. Am. Chem. Soc.* **2003**, *125*, 1788–1795; b) E. Larraneta, J. R. Isasi, *Langmuir* **2012**, *28*, 12457–12462; c) C. Stoffelen, J. Huskens, *Small* **2016**, *12*, 96–119; d) A. Dominski, T. Konieczny, P. Kurcok, *Materials* **2020**, *13*; e) J. Choi, H. Ajiro, *Soft Matter* **2022**, *18*, 8885–8893.
[7] a) A. Harada, M. Kamachi, *Macromolecules* **1990**, *23*, 2821–2823; b) A. Harada, J. Li, M. Kamachi, *Nature* **1992**, *356*, 325–327; c) S. Yamada, Y. Sanada, A. Tamura, N. Yui, K. Sakurai, *Polymer J.* **2015**, *47*, 464–467; d) S. Uenuma, R. Maeda, H. Yokoyama, K. Ito, *Macromolecules* **2019**, *52*, 3881–3887.
[8] a) I. W. Hamley, *Biomacromolecules* **2014**, *15*, 1543–1559; b) H. Acar, J. M. Ting, S. Srivastava, J. L. LaBelle, M. V. Tirrell, *Chem. Soc. Rev.* **2017**, *46*, 6553–6569.
[9] a) L. O. Tjernberg, C. Lilliehook, D. J. E. Callaway, J. Naslund, S. Hahne, J. Thyberg, L. Terenius, C. Nordstedt, *J. Biol. Chem.* **1997**, *272*, 17894–17894; b) L. O. Tjernberg, D. J. E. Callaway, A. Tjernberg, S. Hahne, C. Lilliehöök, L. Terenius, J. Thyberg, C. Nordstedt, *J. Biol. Chem.* **1999**, *274*, 12619–12625; c) M. J. Krysmann, V. Castelletto, A. Kelarakis, I. W. Hamley, R. A. Hule, D. J. Pochan, *Biochemistry* **2008**, *47*, 4597–4605; d) I. W. Hamley *Chem. Rev.* **2012**, *112*, 5147–5192.
[10] a) I. W. Hamley, M. J. Krysmann, V. Castelletto, L. Noirez, *Adv. Mater.* **2008**, *20*, 4394–4397; b) I. W. Hamley, M. J. Krysmann, V. Castelletto, A. Kelarakis, L. Noirez, R. A. Hule, D. Pochan, *Chem. Eur. J.* **2008**, *14*, 11369–11374; c) V. Castelletto, G. E. Newby, Z. Zhu, I. W. Hamley, L. Noirez, *Langmuir* **2010**, *26*, 9986–9996; d) V. Castelletto, G. E. Newby, D. Hermida-Merino, I. W. Hamley, D. Liu, L. Noirez, *Polym. Chem.* **2010**, *1*, 453–459.
[11] a) M. J. Krysmann, V. Castelletto, I. W. Hamley *Soft Matter* **2007**, *3*, 1401–1406; b) M. J. Krysmann, V. Castelletto, J. M. E. McKendrick, I. W. Hamley, C. Stain, P. J. F. Harris, S. M. King, *Langmuir* **2008**, *24*, 8158–8162.
[12] V. Castelletto, I. W. Hamley, P. J. F. Harris, *Biophys. Chem.* **2008**, *138*, 29–35.
[13] N. P. Cowieson, C. J. C. Edwards-Gayle, K. Inoue, N. S. Khunti, J. Doutch, E. Williams, S. Daniels, G. Preece, N. A. Krumpa, J. P. Sutter, M. D. Tully, N. J. Terrill, R. P. Rambo, *J. Synchrotron Radiat.* **2020**, *27*, 1438–1446.
[14] M. D. Tully, J. Kieffer, M. E. Brennich, R. C. Aberdam, J. B. Florial, S. Hutin, M. Oscarsson, A. Beteva, A. Popov, D. Moussaoui, P. Theveneau, G. Papp, J. Gigmes, F. Cipriani, A. McCarthy, C. Zubieta, C. Mueller-Dieckmann, G. Leonard, P. Pernot, *J. Synchrotron Radiat.* **2023**, *30*, 258–266.
[15] C. J. C. Edwards-Gayle, N. Khunti, I. W. Hamley, K. Inoue, N. Cowieson, R. Rambo, *J. Synchrotron Radiat.* **2021**, *28*, 318–321.
[16] a) I. Bressler, J. Kohlbrecher, A. F. Thünemann, *J. Appl. Crystallogr.* **2015**, *48*, 1587–1598; b) J. Kohlbrecher, I. Bressler, *J. Appl. Crystallogr.* **2022**, *55*, 1677–1688.
[17] I. W. Hamley, *Small-Angle Scattering: Theory, Instrumentation, Data and Applications*, Wiley, Chichester, **2021**.
[18] C. Teuchert, C. Michel, F. Hansen, D. Y. Park, H. W. Beckham, G. Wenz, *Macromolecules* **2013**, *46*, 2–7.
[19] J. Pena-Bahamonde, J. J. Atencia, J. Pozuelo, M. P. Tarazona, F. Mendicuti, *Macromol. Chem. Phys.* **2013**, *214*, 2802–2812.
[20] I. N. Topchieva, A. E. Tonelli, I. G. Panova, E. V. Matuchina, F. A. Kalashnikov, V. I. Gerasimov, C. C. Rusa, M. Rusa, M. A. Hunt, *Langmuir* **2004**, *20*, 9036–9043.
[21] a) B. Stuart, *Biological Applications of Infrared Spectroscopy*, Wiley, Chichester, **1997**; b) A. Barth, C. Zscherp, *Quart. Rev. Biophys.* **2002**, *35*, 369–430; c) I. W. Hamley *Angew. Chem.* **2007**, *46*, 8128–8147.
[22] B. Rajbanshi, S. Saha, K. Das, B. K. Barman, S. Sengupta, A. Bhattacharjee, M. N. Roy, *Sci. Rep.* **2018**, *8*.
[23] L. J. Bellamy, *The Infra-Red Spectra of Complex Molecules*, Chapman and Hall, London **1975**.
[24] a) H. LeVine, *Protein Sci.* **1993**, *2*, 404–410; b) H. LeVine, in *Methods in Enzymology, Vol. 309* (Ed.: R. Wetzel), Academic Press, San Diego, **1999**, pp. 274–284; c) M. R. H. Krebs, E. H. C. Bromley, A. M. Donald, *J. Struct. Biol.* **2005**, *149*, 30–37.
[25] A. J. Ryan, S.-M. Mai, J. P. A. Fairclough, I. W. Hamley, C. Booth, *Phys. Chem. Chem. Phys.* **2001**, *3*, 2961–2971.
[26] S.-M. Mai, J. P. A. Fairclough, K. Viras, P. A. Gorry, I. W. Hamley, A. J. Ryan, C. Booth, *Macromolecules* **1997**, *30*, 8392–8400.
[27] T. E. Creighton, *Proteins. Structures and Molecular Properties*, W. H. Freeman, New York, **1993**.

Manuscript received: June 23, 2023
Revised manuscript received: July 28, 2023
Accepted manuscript online: August 2, 2023
Version of record online: ■■, ■■

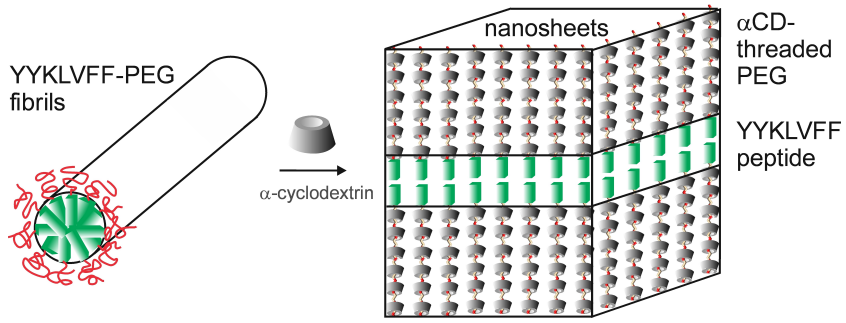

Dr. V. Castelletto, Dr. R. M. Kowalczyk, Dr. J. Seitsonen, Prof. Dr. I. W Hamley**

1 – 9

Tuning the Solution Self-Assembly of a Peptide-PEG (Polyethylene Glycol) Conjugate with α-Cyclodextrin

The influence of alpha-cyclodextrin (αCD) on the aqueous solution self-assembly of peptide-polymer conjugate YYKLVFF-PEG3K is examined. Cryo-TEM and SAXS show that the conjugate self-assembles into β-sheet fibrils in aqueous solution, but complexation with αCD leads to free-floating nanosheets in aqueous solution (with a β-sheet structure). The transition from fibrils to nanosheets is driven by an increase in the number of αCD molecules threaded on the PEG chains, as determined by ^{1}H NMR spectroscopy.